Sex Plant Reprod (2006) 19: 51–62
DOI 10.1007/s00497-006-0021-9

ORIGINAL ARTICLE

Kathleen L. Wilsen · Alenka Lovy-Wheeler
Boris Voigt · Diedrik Menzel · Joseph G. Kunkel
Peter K. Hepler

Imaging the actin cytoskeleton in growing pollen tubes

Received: 27 November 2005 / Accepted: 4 January 2006 / Published online: 7 February 2006

Abstract Given the importance of the actin cytoskeleton to pollen tube growth, we have attempted to decipher its structure, organization and dynamic changes in living, growing pollen tubes of *Nicotiana tabacum* and *Lilium formosanum*, using three different GFP-labeled actin-binding domains. Because the intricate structure of the actin cytoskeleton in rapidly frozen pollen tubes was recently resolved, we now have a clear standard against which to compare the quality of labeling produced by these GFP-labeled probes. While GFP-talin, GFP-ADF and GFP-fimbrin show various aspects of the actin cytoskeleton structure, each marker produces a characteristic pattern of labeling, and none reveals the entire spectrum of actin. Whereas GFP-ADF, and to a lesser extent GFP-talin, label the fringe of actin in the apex, no similar structure is observed with GFP-fimbrin. Further, GFP-ADF only occasionally labels actin cables in the shank of the pollen tube, whereas GFP-fimbrin labels an abundance of fine filaments in this region, and GFP-talin bundles actin into a central cable in the core of the pollen tube surrounded by a few finer elements. High levels of expression of GFP-talin and GFP-fimbrin frequently cause structural rearrangements of the actin cytoskeleton of pollen tubes, and inhibit tip growth in a dose dependent manner. Most notably, GFP-talin results in thick cortical hoops of actin, transverse to the axis of growth, and GFP-fimbrin causes actin filaments to aggregate. Aberrations are seldom seen in pollen tubes expressing GFP-ADF. Although these markers are valuable tools to study the structure of the actin cytoskeleton of growing pollen tubes, given their ability to cause aberrations and to block pollen tube growth, we urge caution in their use.

Electronic Supplementary Material Supplementary material is available for this article at http://dx.doi.org/10.1007/s00497-006-0021-9 and is accessible for authorized users.

Communicated by R. Russell

Financial Source: National Science Foundation grant Nos. MCB-0077599 and MCB-0516852 to PKH EU Research Training Network TIPNET (project HPRN-CT-2002-00265), Brussels, Belgium, to BV

K. L. Wilsen · A. Lovy-Wheeler · P. K. Hepler (✉)
Plant Biology Program, University of Massachusetts,
221 Morrill Science Center South, Amherst,
MA 01003-9297, USA
E-mail: hepler@bio.umass.edu
Tel.: +413-5452083
Fax: +413-5453243

B. Voigt · D. Menzel
Institute of Botany, University of Bonn,
Kirschallee 1, Bonn, Germany

J. G. Kunkel
Biology Department, University of Massachusetts,
221 Morrill Science Center South, Amherst, MA 01003, USA

Present address: K. L. Wilsen
Biological Sciences, University of Northern Colorado,
Ross Hall 2480, Greeley, CO 80639, USA

Introduction

A pollen tube is the tip-growing cell that extends from a pollen grain once it has landed on a receptive stigma. Its function is to navigate the sperm cells through the style and to present them to the ripe ovule. A dynamic actin cytoskeleton is essential for pollen tube growth (Taylor and Hepler 1997; Gibbon et al. 1999; Vidali et al. 2001a). First, acto-myosin drives cytoplasmic streaming and thus the transport of vesicles, which are required for growth at the apex. Second, actin polymerization itself plays an integral role in pollen tube growth, insofar as agents that block actin polymerization, such as profilin, DNAse, cytochalasin-D and latrunculin-B, inhibit pollen tube elongation at a substantially lower concentration than they block cytoplasmic streaming (Vidali et al. 2001a).

A detailed knowledge of the organization of the actin cytoskeleton is thus crucial for our understanding of the process of pollen tube growth. This issue, which has

been recognized for years, has been the focus of numerous studies that have attempted to establish a consistent and clear pattern for actin organization, especially in the apex of the pollen tube (Hepler et al. 2001; Foissner et al. 2002). Unfortunately there is considerable variation in the results, which in large measure has been attributed to the problems of fixing a cell that grows very rapidly, together with the realization that actin microfilaments themselves are extremely fragile cytoplasmic elements, and thus easily disrupted, or even destroyed by commonly used fixation regimens. In a recent study, Lovy-Wheeler et al. (2005), have readdressed this problem and have provided a detailed and consistent image of the structure and organization of actin microfilaments, especially in lily pollen tubes. By stabilizing cell components through rapid freeze fixation, which is known for its ability to preserve cell structure faithfully, and by staining those intact cells with fluorescent antibodies, it has been possible to provide a global view of the organization of the actin cytoskeleton (Fig. 1). Of special note, the confocal images of pollen tubes prepared in this manner consistently reveal the presence of a dense fringe of longitudinally-oriented cortical actin filaments starting 1–5 μm from the apex, and extending for about 5–10 μm. By contrast, actin cables in the pollen tube shank are finer than those seen in the fringe, and are dispersed throughout the pollen tube (Lovy-Wheeler et al. 2005, Fig. 1). With a much more refined image of actin organization in fixed pollen tubes, it becomes important to resolve the structure in living cells, where in addition it is possible to observe actin dynamics directly.

Attempts to resolve the configuration of actin in the pollen tube apex have been made on living cells, but there is much uncertainty and disagreement in the results. Initial studies on live pollen tubes in which small quantities of rhodamine-phalloidin were microinjected, revealed numerous filamentous structures in the shank of the pollen tube, but few in the apex (Miller et al. 1996). However, it has subsequently been determined that phalloidin, while initially labeling F-actin, is progressively sequestered into the vacuole in living cells. Since the pollen tube vacuole consists of a dynamic network of fine interconnected tubules (L. Cárdenas, personal communication), which moves along actin cables, there is a shift in the identity of the stained compartment from F-actin itself, to the filamentous vacuole network. As a consequence, the phalloidin injection method becomes unreliable for depicting the actin cytoskeleton in living cells, especially in the extreme apical domain of the pollen tube.

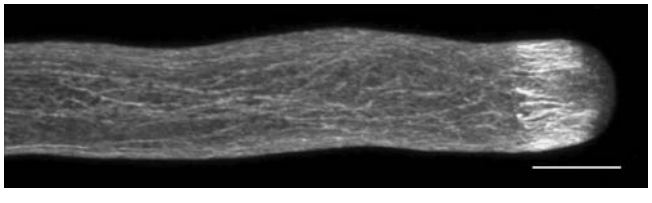

Fig. 1 Actin organization in a rapidly frozen and immunolabeled *L. longiflorum* pollen tube. Image is a projection of a stack of confocal slices. *Bar* 10 μm

Numerous attempts to image the actin cytoskeleton of pollen tubes with GFP-labeled actin have failed, even though a variety of different actin genes have been tested. GFP-actin either fails to incorporate into the native population of actin, giving rise to a uniform fluorescent background signal (unpublished observations), or it labels actin microfilaments, but inhibits pollen tube growth (Kost et al. 1998). Therefore, actin-binding protein based methods of actin visualization are emerging as popular tools to study the actin cytoskeleton in live pollen tubes.

The first of these markers to be developed for use in plant cells was GFP-mTn (Kost et al. 1998), which consists of GFP fused to the actin-binding domain of mouse talin, a protein which has no known homologue in *Arabidopsis thaliana*. Although this technique has generally been regarded to label the actin cytoskeleton in a non-invasive manner (Kost et al. 1998), and expression of GFP-talin is claimed not to affect pollen tube growth or morphology (Fu et al. 2001), it has been noted that expression of GFP-talin may cause actin cables to thicken, cytoplasmic streaming to be retarded, and pollen tube growth to be terminated prematurely (Kost et al. 1998). The observation that *N. tabacum* pollen tubes expressing GFP-talin rarely exceed 600 μm in length, even after 12 h of growth (Laitiainen et al. 2002), shows that GFP-talin expression has an inhibitory effect on pollen tube growth. Furthermore, studies conducted in *Dictyostelium discoideum* using the GFP-tagged talin fragment show that when levels of talin are high, actin is sequestered and cell division is severely hindered (Weber et al. 2002). A recent study conducted on *Arabidiopsis* root hairs shows that the alcohol inducible expression of GFP-talin prevents actin depolymerization and causes pronounced defects in actin organization, resulting in changes of cell shape, termination of growth, and cell death (Ketelaar et al. 2004a). Additional criticism derives from recent studies on root (Wang et al. 2004; Voigt et al. 2005) and shoot tissues (Sheahan et al. 2004) in which it is emphasized that GFP-talin fails to identify all arrays of actin and, furthermore, induces stabilization of actin filaments which may in some cases result in the formation of aberrant actin structures.

Transient expression of GFP-talin in tobacco pollen tubes reveals a ring or collar of actin around the organelle exclusion zone and shows the tip to be depleted of an actin network (Kost et al. 1998). Using an enhanced form of GFP-talin, the presence of F-actin short actin bundles was reported in the extreme apex of tobacco pollen tubes, in addition to the subapical actin collar (Fu et al. 2001). The authors contend that the short actin bundles and the actin collar are two very dynamic groups of actin belonging to the same population, as the appearance of one of these groups is associated with the disappearance of the other.

More recently, GFP fused to the actin depolymerizing protein ADF1, was used to image the actin cytoskeleton of both lily and tobacco pollen tubes (Chen et al. 2002). An actin meshwork, analogous to the previously reported actin collar, but present throughout the thickness of the pollen tube, was observed within the apex.

Given the importance of actin in the regulation of pollen tube growth, we undertook the present study to resolve how F-actin is organized in growing pollen tubes. We evaluated the ability of three different GFP-based markers to reveal the intricate structure of actin in live pollen tubes. For the first time, we are able to compare the images produced by GFP-based probes with a reliable standard, namely images of rapidly frozen pollen tubes immunolabeled with anti-actin (Lovy-Wheeler et al. 2005). In addition to the talin and ADF probes, we include GFP fused to the second actin-binding domain of fimbrin from *A. thaliana* in this study. This probe has been used to image the actin cytoskeleton of plant roots, root hairs, hypocotyls, leaf epidermis, trichomes, guard cells, and mesophyll protoplasts (Sheahan et al. 2004a, b; Voigt et al. 2004; Wang et al. 2004). Our results show that each live cell marker highlights different aspects of the pollen tube actin cytoskeleton, however, no one marker faithfully shows the complete range of actin organization.

Materials and methods

Cell culture

Lilium formosanum was grown from seed in growth chambers and transferred to the greenhouse upon bulb formation. *L. longiflorum* bulbs were kindly donated by the Gloeckner Company and grown in the greenhouse in early Spring. *Nicotiana tabacum* was grown in growth chambers under a standard regimen. Pollen was either used fresh, or frozen at −80°C in the case of *Lilium* and at −20°C in the case of *N. tabacum*. *Lilium* pollen grains were germinated in medium consisting of 15 mM MES, 1.6 mM BO_3H, 1 mM KCl, 0.1 mM $CaCl_2$, and 7% (w/v) sucrose, pH 5.5–6, and *N. tabacum* pollen grains were germinated in medium containing 5 μM $CaCl_2$, 5 μM $Ca(NO_3)_2$, 1 mM $Mg(SO_4)_2$, 0.01% H_3BO_3, and 18% sucrose, pH 6.5–7.0 (Fu et al. 2001). After a germination period of 45 min to 3 h, the pollen tubes were allowed to settle and then mixed on a cover slip with 1.4% (w/v) low melting point agarose in germination medium, at a ratio of 1:1. Excess fluid was wicked away, the agarose was set in the refrigerator for 20 s, and the cells were submerged in pollen germination medium. Pollen tubes recovered for at least 15 min before inspection.

Construct preparation

Two forms of pLAT52::GFP-talin were kindly donated by N.-H. Chua (Kost et al. 1998) and Z. Yang (Fu et al. 2001). The pZmc13::GFP-mTn construct was kindly provided by Hen-ming Wu and Alice Cheung, and consists of the original GFP-mTn construct (Kost et al. 1998) cloned behind the pZmc13 promoter (Hamilton 1998) for expression in lily pollen tubes (Chen et al. 2002). pLAT52::GFP and pZmc13::GFP-LlADF1 were kindly provided by Hen-ming Wu and Alice Cheung (Chen et al. 2002). GFP-fimbrin was amplified from pGFP-FABD2 (Ketelaar et al. 2004b, Voigt et al. 2005), which contains GFP fused to the second actin-binding domain of AtFim1, using the following PCR primers: forward primer, 5′-CCGCGAATTCCCATGGGTAAA GGAGA-3′ and reverse primer, 5′-CCGGGTCGA CACTAGTTCATGACTCGA-3′. PCR products were digested with *Eco*RI and *Sal*I and cloned into pBluescript SKII+ vectors (Stratagene, La Jolla, CA, USA) downstream of the Lat52 (Twell et al. 1990), and Zmc13 promoters (Hamilton 1998), for expression in *N. tabacum* and *Lilium* pollen, respectively. Plasmid DNA was extracted using a QIAprep Spin Miniprep Kit (Qiagen, Inc., Valencia, CA, USA) and ethanol precipitated to a final concentration of 1 μg/μl.

Rapid freeze fixation and immunolabeling

Lilium. longiflorum pollen tubes where surface germinated, plunge frozen, and freeze-substituted in dry acetone, as reported by Lovy-Wheeler et al. (2005). After fixation, actin was stained with a mouse anti-actin antibody, raised against chicken gizzard actin (Chemicon, Temecular, CA, USA), and a secondary Cy-3 goat anti-actin antibody (Jackson ImmunoResearch Laboratories, Inc, West Grove, PA, USA), as previously described (Lovy-Wheeler et al. 2005).

Microprojectile Bombardment

Plasmid DNA was coated onto 3 mg tungsten particles (diameter 1.1 μm, Bio-Rad Laboratories, Hercules, CA, USA), following the manufacturer's guidelines. Since the tungsten particles were divided between two macrocarriers (Bio-Rad Laboratories, Hercules, CA, USA), a microprojectile aliquot is defined here as 1.5 mg. Generally, 0.5 μg plasmid DNA was used per microprojectile aliquot for expression in *N. tabacum* pollen, and 1 μg DNA was used for expression in *Lilium* pollen. For the concentration range experiment, 0.25, 0.5, 1, 2.5 and 5 μg DNA were used per microprojectile aliquot. Approximately 10 mg of pollen was hydrated in 100 μl germination medium for 5 min before bombardment, and plated onto a 25 mm MF-Millipore membrane (Millipore, Bedford, MA, USA), which was placed on a piece of moist Whatman filter paper in a petri dish. In the concentration range study, several frozen aliquots of pollen were mixed together and then re-aliquoted to produce a uniform sample of pollen for each of the five bombardments performed on a given day. Pollen grains were transformed by means of microprojectile

bombardment, using a Bio-Rad helium-driven Biolistic PDS-1000 with 1100-psi rupture discs. The microcarrier launch assembly was positioned in the second slot from the top, and the hydrated pollen in the slot below it. Each sample of pollen was bombarded twice, i.e. with both microprojectile aliquots, delivering a total of 3 mg tungsten. Bombarded pollen was transferred into an eppendorf tube with 1 ml germination medium and allowed to germinate on a rotor at room temperature. For regular imaging, pollen tubes were immobilized on 1.4% (w/v) low-melting point agarose about 3 h after bombardment and inspected 4–9 h after bombardment. In the concentration range study, pollen tubes were removed from the rotor 5 h post bombardment and placed in the refrigerator to stop further growth. Since transformation efficiency is low, about 100 µl of pollen was plated between two large coverslips (35×50 mm) to facilitate screening. A similar analysis was not performed on *Lilium* pollen, as pollen tubes are too long and entangled to analyze in this manner after 5 h of growth.

Image acquisition and processing

Confocal images were collected on a Zeiss 510 META laser scanning confocal microscope, using either a plan-neofluor 10X/0.3 N.A. dry objective or a plan-apochromat 63X/1.4 N.A. oil immersion objective. GFP images were acquired using an excitation of 488 nm of the argon laser, and an emission of LP505. Time-series intervals were taken of the medial plane at 3–8 s intervals, and the pollen tubes presented were growing at good average rates at the time of imaging. Z-series images were collected at approximately 1 µm intervals and projected by LSM 5 Image Browser software. This technique was only used to image pollen tubes that had stopped growing, either due to rapid freeze fixation, or to stabilization of the actin cytoskeleton by a GFP-based marker.The clarity of the images in Fig. 4 was improved using the median filter function in Metamorph (Universal Imaging, Downington, PA, USA). For the concentration range studies, transformed pollen tubes were identified using epifluorescence microscopy (dichroic at 495LP, emission bandpass at 515/30 nm). Cells were excited using a DG-4 ultra high speed wavelength switcher system as an illumination source (Sutter Instruments), with a 175 W ozone-free xenon lamp. Images were acquired with a CCD camera (Quantix Cool Snap HQ) coupled to a Nikon TE300 inverted microscope with a 10X/0.3 N.A. dry objective lens and pollen tubes were analyzed using functions on MetaMorph / MetaFluor software (Universal Imaging). Twenty-five transformed pollen tubes were observed and measured for each DNA concentration tested. The average growth rate was calculated by dividing the average length of the pollen tubes by the time of growth (i.e., time elapsed from bombardment to imaging). On a given day, 25 non-transformed pollen tubes were measured as a control. The lengths of transformed pollen tubes were normalized against the control value to minimize differences between experiments conducted on different days with different batches of pollen.

Results

Fluorescence patterns in cells expressing different actin-binding proteins

We transiently expressed GFP-talin and GFP-fimbrin in both *Lilium* (lily) and *N. tabacum* (tobacco) pollen tubes, and GFP-ADF in lily pollen, by means of microprojectile bombardment. Since Chen et al. (2002) have extensively examined the use of GFP-NtADF1 as a

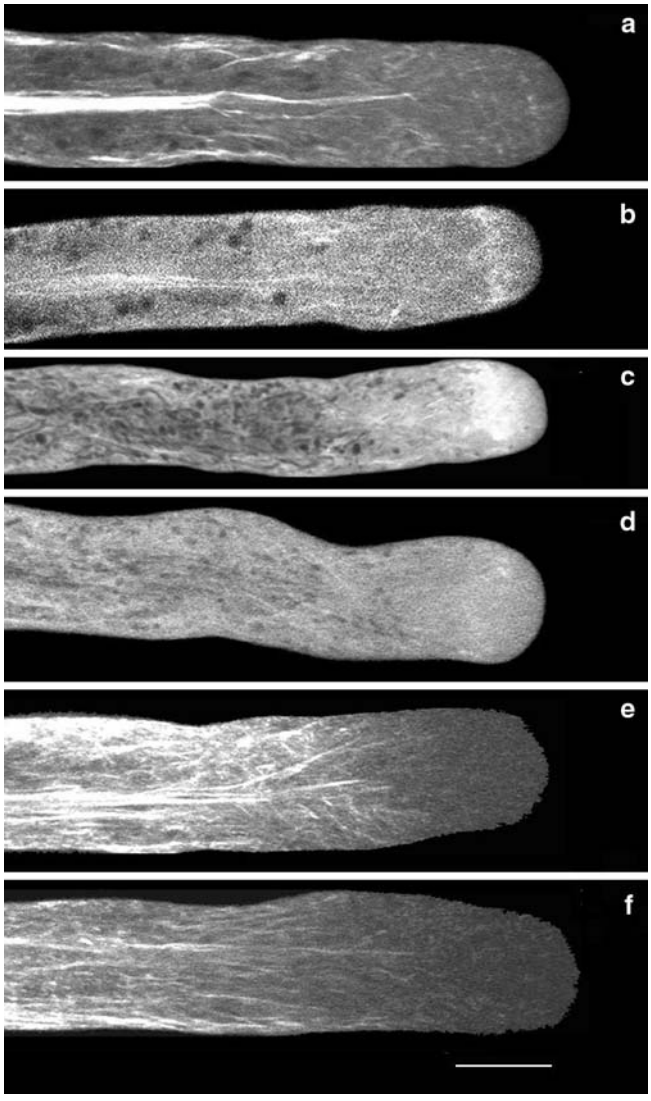

Fig. 2 Confocal micrographs of actin labeling in *Lilium* pollen tubes. Typical patterns of actin labeling in pollen tubes expressing GFP-talin (**a**, **b**), GFP-ADF (**c**, **d**), and GFP-fimbrin (**e**, **f**). The pollen tube in (**b**) is from *L. longliflorum*, whereas the others are all from *L. formosanum*. Images are roughly medial sections. *Bar* 10 µm

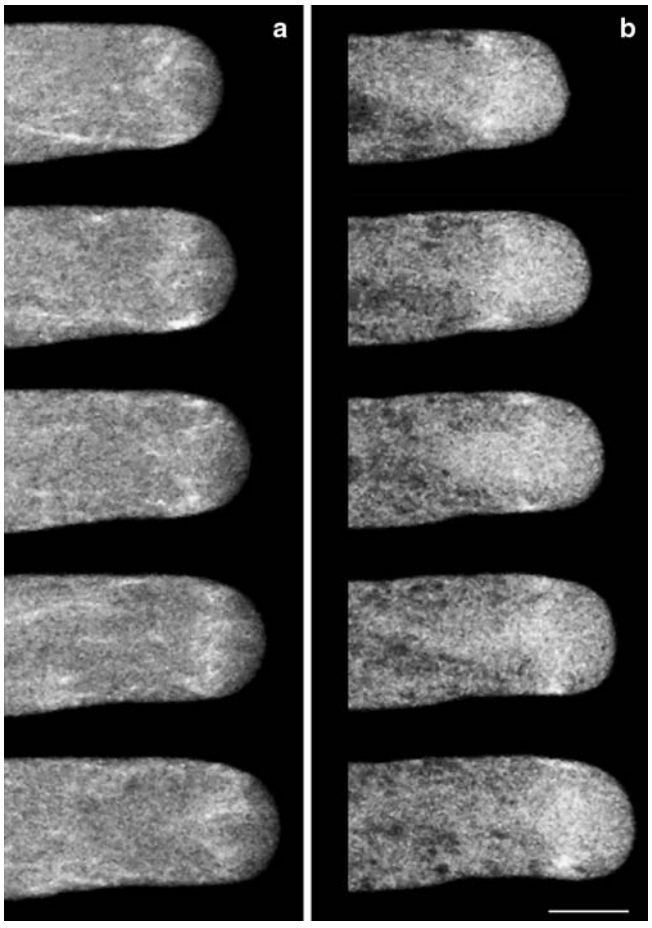

Fig. 3 The disposition of actin in the apex undergoes subtle changes in intensity and position relative to the apex. Medial confocal sections of a *L. longiflorum* pollen tube expressing GFP-talin (**A**) and of a *L. formosanum* pollen tube expressing GFP-ADF1 (**B**). Successive images in each vertical panel were acquired at ~7 s intervals. *Bar* 10 μm

marker of actin in tobacco pollen tubes we have not repeated those studies here. In studies with GFP-talin involving tobacco pollen tubes, we used two different constructs interchangeably: GFP-mTn (Kost et al. 1998) and enhanced GFP-talin (Fu et al. 2001). We did not find a significant difference in signal quality or labeling pattern. In each instance, we found that the pattern of labeling produced by a specific marker is very similar in lily and tobacco pollen tubes; however, when compared to tobacco, lily pollen tubes grow an order of magnitude faster, and provide better spatial resolution.

Rapidly frozen pollen tubes stained with anti-actin antibodies (Fig. 1, Lovy-Wheeler et al. 2005) provide a good standard for evaluating the accuracy of the GFP-based probes.

A medial optical section of pollen tubes labeled with GFP-talin, frequently reveals a thick central bundle of actin filaments in the shank of the pollen tube (Fig. 2a, b, and supplemental material, movie 1). This bundle of actin is also prominent at the widefield level and appears to undergo a marked retrograde motion, as do the vesicles in this region (supplemental material, movie 2 and 3). A faintly stained transverse band of actin is frequently present approximately 2–5 μm behind the apex of growing pollen tubes transformed with GFP-talin (Fig. 3 panel A, supplemental material, movie 1, 2 and 3). Although there is some labeling in the core of the pollen tube, the signal at the cortex dominates. This band is often not apparent (Fig. 2a), or only weakly so (Figs. 2b, 4a, b) in confocal sections. Although distinct actin filaments are not discernable within the band, based on its position and structure we believe that it is an element of the dense actin fringe observed with phalloidin and actin antibody labeling (Lovy-Wheeler et al. 2005, Fig. 1).

We next transformed lily pollen with GFP-ADF (provided by Hen-ming Wu and Alice Cheung), from *L. longiflorum* (Chen et al. 2002). Due to the small size of LlADF1 (544 bp), the entire gene was included in the GFP construct. Expression of GFP-ADF in lily pollen tubes reveals the actin fringe (Fig. 2c, d); however, this is observed in fewer than half of the transformed cells. Again, as with GFP-talin, the filamentous nature of the cortical fringe is not depicted in the live cell imaging. The actin fringe appears brightest at the edges of the cell, but is evident in medial optical sections (Figs. 2c, d, 3 panel B, and supplemental material, movie 4). By contrast, the actin fringe detected in the apex of immunolabeled pollen tubes is almost entirely cortical (Lovy-Wheeler et al. 2005). With GFP-ADF, we also only rarely see labeling of filaments in the shank of the pollen tube, and when these elements are apparent, they are sparse and variable (supplemental material, movie 4). More frequently, there is a diffuse background fluorescence, which may either be attributed to free GFP-ADF, or to an association of the fluorescent protein with G-actin. The diffuse nature of the GFP-ADF signal in the shank can be further appreciated by its ability to outline the filamentous forms of vacuoles (Fig. 2c).

Because both the labeling intensity in the apex and the distance of the fringe from the tip fluctuate during pollen tube growth when using either GFP-talin or GFP-ADF (Fig. 3), we made an attempt to discern if there is a repeating pattern that correlates with the well known oscillation in growth rate. We made a variety of measurements including fluorescence intensity in the extreme apex, fluorescence intensity in the region of the fringe, distance of the fringe from the apex, and distance of the cortical contact points of the fringe to the apex. However, attempts to detect a systematic change or oscillation in apical actin were unsuccessful due to the high level of background fluorescence. Furthermore, we found that GFP expression alone produced fluctuations of fluorescence intensity.

Finally, we constructed GFP-fimbrin, a fusion of GFP with the second actin-binding domain of fimbrin1 from *A. thaliana*, in vectors for expression in both lily and tobacco pollen tubes. At the wide field microscope level, the fluorescence signal comes to an abrupt halt at the base of the clear zone, leaving the apex dark. Quite

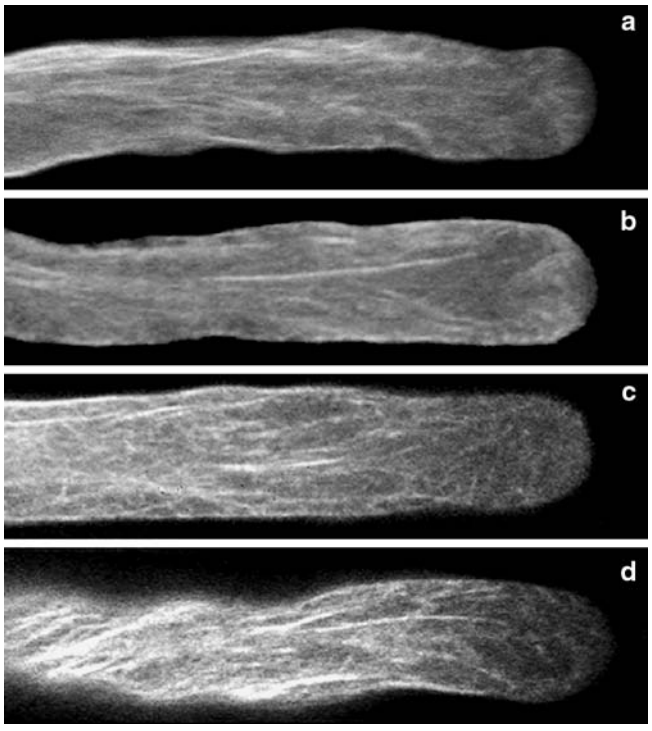

Fig. 4 Confocal micrographs of *N. tabacum* pollen tubes expressing moderate levels of GFP-based actin marker. Medial confocal planes of pollen tube tips probed with GFP-talin (**a**, **b**) and GFP-fimbrin (**c**, **d**). Actin filaments in the shank have a slight helical twist, as seen in pollen tube (**d**), which is not lying quite flat. *Bar* 10 μm

similarly, confocal images present the clear zone of lily pollen tubes expressing GFP-fimbrin as being largely devoid of filamentous actin (Fig. 2e, f). Although fine filaments of actin occasionally extend into the clear zone, no fringe of actin is observed within this region. Due to the smaller size of *N. tabacum* pollen, which has a clear zone of just a few microns, it is hard to determine the exact location of labeling. However, in contrast to studies with GFP-ADF1, we do not see a consistent labeling pattern in the apex, either at the confocal or the widefield level. Instead, the confocal sections of pollen tubes expressing GFP-fimbrin, reveal that the region just distal to the clear zone is packed with numerous fine hair-like bundles of actin (Figs. 2e, f, 4c, d, and supplemental material, movie 5).

Expression of GFP-talin and GFP-fimbrin affects pollen tube growth and morphology

Since it has been established that NtADF1 inhibits pollen tube growth in a dose-dependent manner (Chen et al. 2002), we decided to quantify the effect on pollen tube growth of increasing the concentration of GFP-talin and GFP-fimbrin DNA used per bombardment. We transformed tobacco pollen grains with a range of DNA concentrations and measured the length of transformed pollen tubes after a five hour germination period (Fig. 5). The results of the growth study are expressed as normalized growth rates, obtained by dividing the average growth rate of each transformed pollen tube by the average growth rate of non-transformed pollen tubes in the sample, to minimize variability due to differences between experiments conducted on different days and with different batches of pollen. The DNA concentrations tested here (0.25–5 μg plasmid DNA per 1.5 mg microprojectile particle aliquot) span the range of concentrations used in previous transient expression studies using GFP-talin. Thus, Kost et al. (1998) coated 1.5 mg of gold particles with 2.5–5 μg of plasmid DNA (B. Kost, personal communication), whereas Fu et al. (2001) coated 0.5 mg of gold particles with 0.8 μg of DNA. Compared with GFP controls, both GFP-talin and GFP-fimbrin inhibit pollen tube growth above concentrations of 0.25 μg DNA per tungsten aliquot, with the effect being most significant at concentrations of 5 μg. Further, GFP-fimbrin has a more severe effect on pollen tube growth than GFP-talin (Fig. 5).

GFP-marker expression may also alter the structure of the actin cytoskeleton in pollen tubes. It has previously been noted that very high levels of GFP-NtADF1 expression result in highly bundled or patchy regions of actin (Chen et al. 2002). Here, we find that GFP-talin and GFP-fimbrin are prone to induce aberrant actin rearrangements in pollen tubes, and that each marker produces a characteristic pattern of aberration. Since these structures are more likely to be observed in older pollen tubes, they probably form when the GFP-labeled marker accumulates inside the cell above a certain threshold level. Each bombardment yields a range of expression levels, and even the lowest concentrations of transforming DNA tested give rise to a percentage of pollen tubes with obvious deviations.

As already mentioned, expression of GFP-talin frequently labels a thick central bundle of actin in the core of both *Lilium* and *N. tabacum* pollen tubes (Fig. 2a, b). Since such a structure is never seen in pollen tubes that have been rapidly frozen and immunolabeled (Lovy-Wheeler et al. 2005, Fig. 1), we consider it to be an effect of GFP-talin. Despite bundling of actin in the shank, pollen tubes continue to exhibit oscillatory growth, although the rate of elongation may be diminished. For example, the cell shown in Fig. 2a, which has a very prominent central actin bundle, is growing at 0.1 μm/s, or half the rate of the cell shown in Fig. 2b.

A more striking effect of GFP-talin expression is the emergence of large coils of actin (Fig. 6a–c). These aberrant structures are most frequently observed in the apex of the pollen tube, specifically in the region normally occupied by the dense fringe of actin (Fig. 6a, b), but whereas elements of the fringe are parallel to the axis of growth, the coils of actin are oriented transverse to it. However, they may also occur in the shank of the pollen tube (Fig. 6c). As demonstrated by the medial optical section (Fig. 6b) of a projection of a stack of confocal images (Fig. 6a), actin coils are strictly cortical. By the time these structures are visible, pollen tube growth has

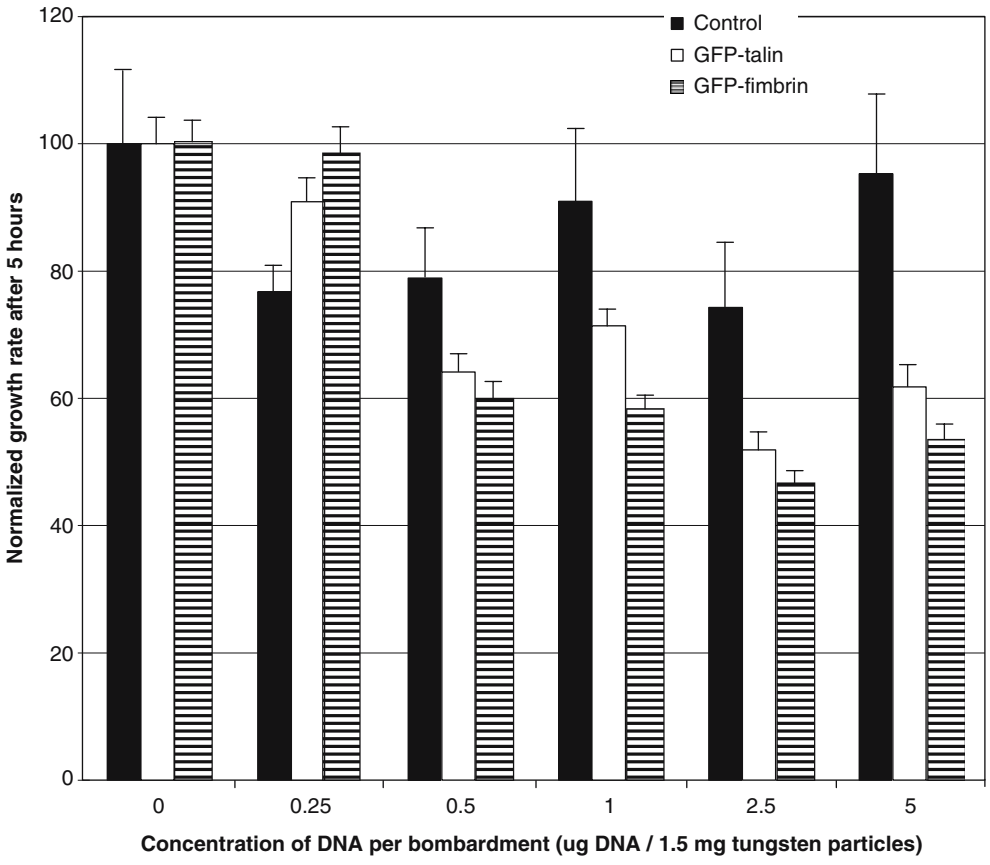

Fig. 5 The growth rate of *N. tabacum* pollen tubes expressing GFP-talin (*square*) or GFP-fimbrin (*striped square*) is inhibited in a dose-dependent manner. Pollen tubes transformed with GFP were used as a control (*filled square*). *Bars* standard error. $n = 25$

either slowed down significantly, or ceased completely. These coiled structures occur frequently in *N. tabacum* pollen tubes expressing GFP-talin (Table 1): after a 5 h growth period, they are present in 8% of pollen tubes transformed with 0.25 μg GFP-talin DNA per 1.5 mg microprojectile particle aliquot, and in 44% of pollen tubes transformed with 5 μg of DNA per aliquot. Please note, however, that these values are an underestimate since they do not include the tubes showing large cables of actin in the shank of the pollen tube. Interestingly, for GFP-talin, both the percentage of pollen tubes exhibiting cortical hoops of actin (Table 1) and the inhibitory effect on pollen tube growth (Fig. 5) are proportional to the concentration of transforming DNA. For instance, when bombarding with 5 μg DNA per microprojectile aliquot, growth rate is inhibited by 38.2%, and 44% of

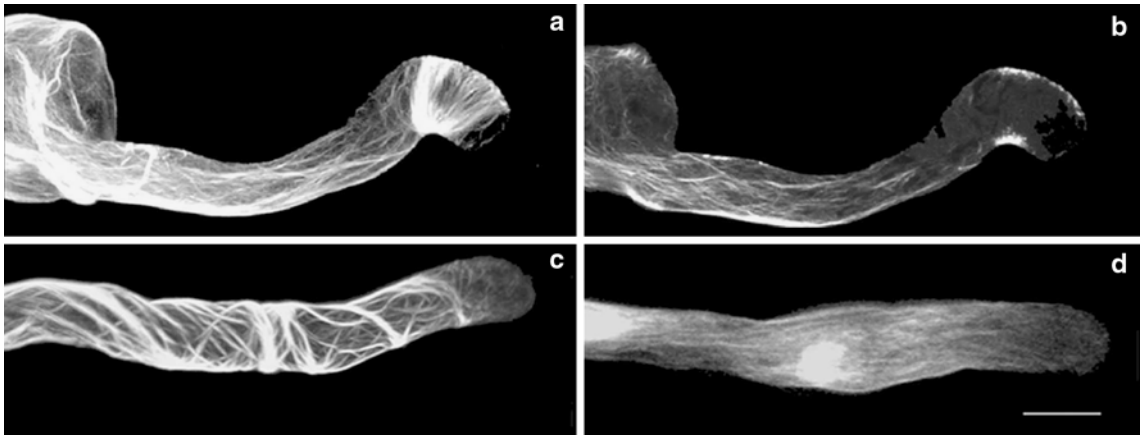

Fig. 6 Common actin cytoskeleton rearrangements caused by high levels of expression of GFP-talin or GFP-fimbrin in *N. tabacum* pollen tubes. Transverse hoops of actin typically occur near the apex of pollen tubes (**a**, **b**), but may also occur at points along the shank of the pollen tube (**c**). A medial slice (**b**) taken from a stack of confocal images (projection shown in a) illustrates that these transverse hoops of actin are cortical. Excessive GFP-fimbrin results in aggregates of actin (**d**). Images (**a**), (**c**), and (**d**) are projections of a *z*-series. *Bar* 10 μm

Table 1 Percentage of aberrant pollen tubes per bombardment, over a range of DNA concentrations

Quantity DNA (μg)	0.25	0.5	1.0	2.5	5
GFP-talin (%)	8	36.67	25	42	44
GFP-fimbrin (%)	72	61.54	76	66.67	86.67

In the case of GFP-talin, only pollen tubes exhibiting cortical hoops of actin were scored. If the occurrence of thick central cables of actin were to be included in this survey, the values would be much higher. For GFP-fimbrin, pollen tubes with large actin aggregates were scored

the observed pollen tubes exhibit abnormalities of the actin cytoskeleton. Thus, pollen tube growth appears to be sensitive to aberrations in apical actin. Although both GFP-talin and the enhanced GFP-talin construct give rise to cortical hoops in *N. tabacum* pollen tubes, we have only seen them once in a *L. formosanum* pollen tube.

Less frequently than the coils, pollen tubes expressing GFP-talin may exhibit cables that appear to have broken (Fig. 7a), and small ring-like structures of actin that move about the pollen tube (Fig. 7b, c). The rings appear to arise from broken actin filaments in the shank of the pollen tube, and several rings may occur in a single pollen tube. Similar rings have also been observed in *N. tabacum* pollen tubes (not shown).

We have only rarely seen evidence of aberrant structures in lily pollen tubes expressing GFP-ADF. In just one case, we observed degraded patches of actin in a *L. formosanum* pollen tube expressing GFP-ADF (Fig. 7d). This particular pollen tube had exceptionally good labeling of actin filaments further down the shank, but its growth was inhibited. A few times we observed very bright diffuse labeling throughout the apex of pollen tubes transformed with high levels of DNA; however, these pollen tubes were growing at very low average rates and were tuberous in shape.

Expression of GFP-fimbrin commonly produces yet a different set of structural rearrangements of actin (Figs. 6d, 7e), in both *L. formosanum* and *N. tabacum* pollen. Actin bundles in the shank of the pollen tube gradually fuse together at localized points, and develop into large aggregates of F-actin. It has previously been reported that AtFim1 transforms plant actin into gelled aggregates in vitro (Kovar et al. 2000). Here it appears that expression of GFP-fimbrin produces similar structures in growing pollen tubes. Similar aggregates of actin have also been described in *D. discoideum* amoebae treated with phalloidin or jasplakinolide (Lee et al. 1998), and in pollen tubes treated with jasplakinolide (Cárdenas et al. 2005). The aggregates are highly variable in size; they may either form small patches of actin (Figs. 6d, 7e), or large conglomerates that almost span the width of the pollen tube (not shown). The actin aggregates usually do not invade the extreme apex of the pollen tube. At the earliest stages of actin bundle fusion, pollen tubes are able to maintain good average rates of growth, but by the time distinct aggregates are visible, growth has either slowed significantly or stopped completely.

The percentage of aberrations occurring in pollen tubes expressing GFP-fimbrin remains consistently high

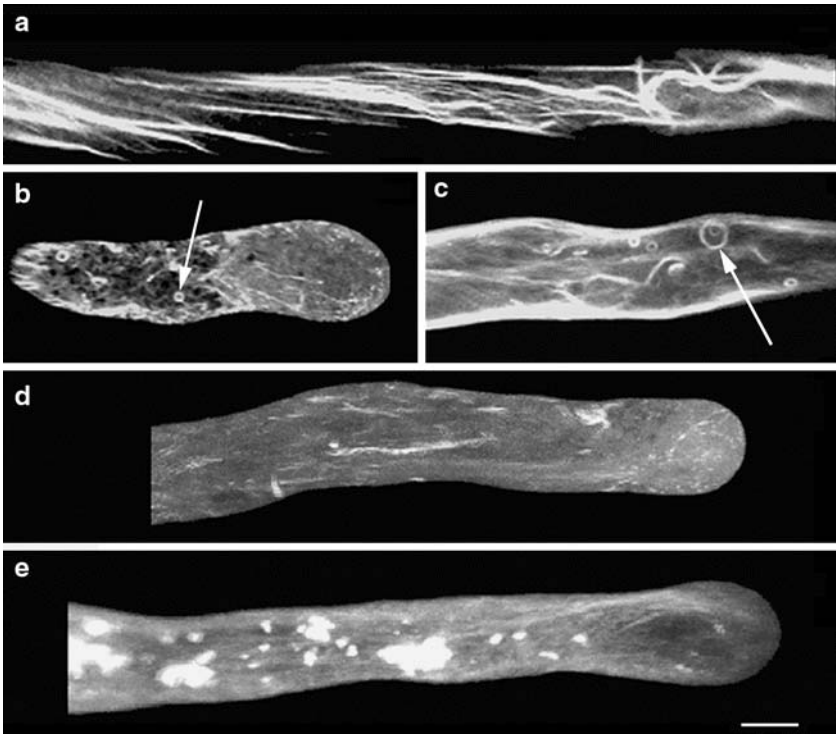

Fig. 7 Artifacts found in *L. formosanum* pollen tubes expressing high levels of GFP-based markers. GFP-talin expression may result in cortical transverse snapping of actin cables (**a**), or the formation of small mobile rings of actin (**b** and **c**, examples indicated by *arrows*). GFP-ADF1 expression can lead to actin filament decay (**d**). GFP-fimbrin expression frequently produces large aggregates of actin within the pollen tube (**d**). Image (**d** and **e**) are projections of a *z*-series, whereas the other images are single confocal slices. *Bar* 10 μm

over the range of DNA concentrations tested (Table 1), whereas the inhibitory effect on pollen tube growth is greatest at higher transforming concentrations (Fig. 5). Therefore, pollen tubes are somewhat able to tolerate the artifacts caused by high levels of GFP-fimbrin expression, most probably because fimbrin predominantly decorates elements of actin in the shank of the pollen tube, which are presumably less crucial to the process of pollen tube growth than elements within the apical fringe of actin.

Discussion

Given the central role that actin plays in the growth of the pollen tube, it is essential that we have a thorough knowledge of its structural organization and dynamic transformations in living cells. Here, three different fluorescent probes have been used to image the actin cytoskeleton of living pollen tubes. However, three distinct views have been obtained, and not one entirely conforms to the structure observed in optimally fixed pollen tubes (Lovy-Wheeler et al. 2005). This may be due to a preference of these markers for a particular isovariant of actin, of which there are five in *A. thaliana* pollen tubes (Kandasamy et al. 1999), or for actin with specific physical properties. Alternatively, the binding properties of these probes may significantly be altered by the concentration of certain ions, such as calcium and protons, which are known to vary in the apical region of growing pollen tubes (Holdaway-Clarke and Hepler 2003). Furthermore, it must be emphasized that these probes are actin-binding proteins, and not actin. Therefore the images represent the distribution of the particular actin-binding protein, and this does not necessarily transcribe into a faithful account of actin distribution.

An important feature of optimally fixed pollen tubes is the presence of a cortical fringe of actin, located just behind the pollen tube tip within the clear zone (Lovy-Wheeler et al. 2005; Fig. 1). Although this fringe has only occasionally been reported in previous studies, the high quality of preservation rendered by rapid freeze fixation allows the fringe to be seen in virtually every pollen tube examined. Furthermore, the failure of older, conventional methods to routinely preserve this structure lends support to the notion that it is a fragile, dynamic structure, easily deformed or destroyed. The location of the fringe suggests that it is involved in actin assembly and turnover, and thus quite likely it participates in the process of growth itself.

Importantly, GFP-ADF and GFP-talin detect this structure. However, there are significant differences between the structure as visualized in living cells and in fixed cells (Lovy-Wheeler et al. 2005). The live cell probes, for example, do not reveal the fibrillar structure of the cortical fringe. In addition they often produce a signal in every plane throughout the pollen tube, whereas the cells prepared by rapid freeze fixation invariably show the actin fringe to be located in the cortex of the cell. Chen et al. (2002) have clearly reported that the fluorescent signal from GFP-ADF occurs throughout the thickness of the pollen tube and refer to this as a mesh, rather than a collar or a fringe. When labeling *L. formosanum* pollen tubes, GFP-ADF frequently produces a stronger signal at the edge of the cell than in the interior. The finding that GFP-ADF often gives rise to a uniform signal may be explained by the fact that ADF is uniformly distributed throughout the pollen tube, as revealed by antibody labeling in *Narcissus* pollen tubes (Allwood et al. 2002). Perhaps, when levels of ADF are elevated above a certain threshold, they preferentially associate with actin in the region of the apical fringe.

In summary, therefore, we think that principal ADF activity occurs in the cell cortex, and that it marks regions of active actin polymerization and turnover, which must accompany or indeed anticipate pollen tube growth. In this regard it is particularly pertinent that ADF1 is well known for its association with actin remodeling in other systems (Kuhn et al. 2000). It is additionally relevant that the position of the fringe corresponds to the location of the alkaline band (Feijó et al. 1999); thus the physiological conditions are primed to enhance the actin remodeling activity of ADF (Chen et al. 2002). It is therefore possible that expression of GFP-ADF enhances actin turnover in this region, generating more short fragments of actin and providing an over-representation of actin fragments than would normally be present in the fringe.

With both GFP-ADF and GFP-talin the fringe appears to undergo changes in conformation, distance from the apex, and intensity, most probably correlating with changes in pollen tube growth rate. However, despite considerable effort, we have not been able to deconvolve the changes of fluorescence into a meaningful understanding of actin dynamics. First, the high level of background fluorescence makes it difficult to extract a clear signal. Second, there are other events, notably oscillations in pH in the apical domain (Feijó et al. 1999), and changes in the accessible volume in the clear zone, which may account for fluctuations in signal intensity. Since GFP is sensitive to pH (Tsien 1998), the presence of oscillatory domains of pH could readily obscure or dominate a signal derived from the purported changes in actin. In addition to the pH changes, there are changes in accessible volume due to the periodic motion of Golgi-derived membrane vesicles and elements of the ER in the pollen tube apex (Parton et al. 2001; Parton et al. 2003). These too could have a profound effect on the amount of fluorescence from a single wavelength indicator. Although there is one report on the occurrence of actin oscillations in the apex of tobacco pollen tubes (Fu et al. 2001), those data must be considered with caution because the authors did not consider issues of pH and accessible volume. Our observation that the fluorescence from free GFP oscillates indicates that changes in GFP signal occur that are independent of actin binding.

GFP-fimbrin generously labels fine bundles of actin in the shank of the pollen tube. By comparison, pollen tubes transiently expressing GFP-ADF only rarely exhibit the occasional filament of actin in the shank, and those expressing GFP-talin often reveal a prominent central bundle of actin surrounded by a few fine filaments. It is possible that the abundance of actin bundles labeled with GFP-fimbrin is the result of the construct somehow altering the structure of the actin cytoskeleton. Co-injection of stamen hair cells with AtFim1 and fluorescent phalloidin labels much finer bundles of actin than fluorescent phalloidin alone (Kovar et al. 2001). Kovar et al. (2001), suggest that this phenomenon may be an artifact, and that AtFim1 may be inducing polymerization of actin or splaying apart pre-existing bundles of F-actin. However, considering the similarity between GFP-fimbrin and those pollen tubes that have been rapidly frozen and labeled with anti-actin (Lovy-Wheeler et al. 2005), we conclude that GFP-fimbrin produces the most accurate image of actin in the shank of live pollen tubes.

An important aspect of this study is the demonstration that expression of GFP-labeled actin-binding domains may inhibit pollen tube growth and cause structural rearrangements of the actin cytoskeleton. Even with relatively low concentrations of transforming DNA, a percentage of transformants exhibits actin cytoskeleton aberrations. This is significant, because the isolated C-terminal of talin has been used as an "unobtrusive" marker of the actin cytoskeleton (Kost et al. 1998; Fu et al. 2001). However, it clearly is not an "unobtrusive" marker since it routinely produces a variety of defects in actin cytoskeleton structure and inhibits pollen tube growth. Perhaps this is to be expected, as it has previously been demonstrated that the exact same 197 amino acid C-terminal region of talin present in the GFP-talin construct spontaneously forms homodimers when expressed at physiological conditions, and cross-links F-actin into short bundles. Furthermore, this truncated version of talin binds to actin so strongly that it displaces native talin from its binding site at very low concentrations (McCann and Craig 1997). It is therefore conceivable that, when GFP-talin reaches a certain level of expression in pollen tubes, it is able to override native actin-binding protein activity and cross-link short actin bundles in the apex into stable structures that undergo coiling. Structural anomalies caused by GFP-talin appear to be present in previous studies. For example, coils of actin were reported in pollen tubes overexpressing Rop, based on studies using GFP-talin as an actin marker (Fu et al. 2001). Given the propensity for GFP-talin to generate pronounced structural rearrangements, including especially transverse coils or hoops, it is therefore an unresolved question whether the images reported by Fu et al. (2001) were primarily due to Rop1 overexpression or whether GFP-talin had the dominant impact. Similarly, steep helical and small ring-like structures of actin found in *N. tabacum* pollen tubes were attributed to oryzalin treatment, when GFP-talin was being used as a marker for actin (Laitiainen et al. 2002).

GFP-talin is not alone in its ability to modify the actin cytoskeleton. Aggregates of actin resulting from high levels of GFP-fimbrin expression may either result from excessive actin filament stabilization, or from unusual intrafilament binding and buckling. Pollen tubes continue to grow normally in the presence of moderate levels of aggregation. This is possibly because GFP-fimbrin is ineffective at binding to the cortical actin fringe within the clear zone, a region that is crucial for tip growth to occur. An isolated actin-binding domain of human T-fimbrin induces a conformational shift in an actin filament upon merely binding to it, a change that is likely to prevent other actin-binding proteins from binding in the vicinity (Hanein et al. 1997). Expression of a single actin-binding domain of AtFim1 may therefore prevent native actin-binding proteins from binding to the actin cables in the shank of the pollen tube, and result in structural rearrangements. When taken together, GFP-fimbrin emerges as the least effective marker to study apical actin, and therefore actin dynamics, in growing pollen tubes. These observations in the pollen tube stand in contrast to recent reports which promote this same GFP-fimbrin (ABD2) construct as an efficacious probe for dynamic actin networks in a variety of plant tissues, including the tip-growing root hair (Sheahan et al. 2004; Ketelaar et al. 2004b; Voigt et al. 2005).

Due to the negative impact of GFP-based markers on pollen tube growth and actin cytoskeleton structure, we recommend bombarding with the lowest concentration of DNA that still provides a signal strong enough for the imaging technique being used. It is important to note that even the lowest concentrations of transforming DNA tested produce a range of expression levels and result in a fraction of aberrant pollen tubes. Inducible promoters may be an effective mechanism to regulate expression levels of GFP-markers in stable transgenic lines.

Perhaps the most effective approach is to use a variety of different actin markers when studying changes in the actin cytoskeleton. For instance, had GFP-ADF1 been used as an actin marker in the Rop1 overexpression study (Fu et al. 2001) the results might have been unambiguous, as GFP-ADF1 by itself rarely if ever induces the formation of transverse coils of actin. Furthermore, in general, structural aberrations are less likely to develop in lily pollen tubes. This may be due to differences in the strength of the promoters used in these two systems, or to dilution of the probe in the larger accessible volume of the lily pollen tube.

Although the fixation methods, especially rapid freeze fixation, followed by immunostaining (Lovy-Wheeler et al. 2005), offer the most complete view of the pollen tube actin cytoskeleton, they provide just a snapshot and do not reveal how the pollen tube actin cytoskeleton is remodeled during pollen tube growth. The GFP-based markers used in live-cell studies preferentially label distinct elements of the actin cytoskeleton and thus

provide only limited details of its structure and dynamic changes. Furthermore, these markers are prone to produce aberrant actin structures and inhibit pollen tube growth, especially in the case of tobacco pollen. It is unfortunate that GFP-actin has not worked thus far; perhaps future efforts on this approach, or possibly an actin-binding protein or domain that has not yet been tested, will yield an efficacious live cell probe. The ideal probe would detect all arrays of actin present in the growing pollen tube, without interfering with normal actin dynamics. Nonetheless, much may be learnt about the actin cytoskeleton using a combination of these markers currently available if one validates the resulting images by comparison with the best available standard produced by optimally fixed pollen tubes (Lovy-Wheeler et al. 2005) and excludes the pollen tubes exhibiting characteristic aberrations.

Acknowledgements We thank Nam-Hai Chua, Zhenbiao Yang, Alice Cheung and Hen-ming Wu for providing us with constructs, and the Gloeckner Company for the donation of *L. longiflorum* bulbs. We thank Alice Cheung for the contribution of Fig. 6a and b. This research was supported by the National Science Foundation grant Nos. MCB-0077599 and MCB-0516852 to PKH and by the EU Research Training Network TIPNET (Project HPRN-CT-2002–00265), from Brussels, Belgium, to BV. We acknowledge the National Science Foundation Grant No. BBS 8714235 that supports the UMASS Central Microscopy Facility, where all confocal images were acquired. Finally, we acknowledge the David Delisle Research Grant, of the Plant Biology Graduate Program at UMASS, for its support.

References

Allwood E, Anthony R, Smertenko A, Reichelt S, Drøbak B, Doonan J, Weeds A, Hussey P (2002) Regulation of the pollen-specific actin-depolymerizing factor LlADF1. Plant Cell 14:2915–2927. DOI 10.1105/tpc.005363

Cárdenas L, Lovy-Wheeler A, Wilsen KL, Hepler PK (2005) Actin polymerization promotes the reversal of streaming in the apex of pollen tubes. Cell Motil Cytoskel 61:112–127. DOI 10.1002/cm.20068

Chen CY, Wong EI, Vidali L, Estavillo A, Hepler PK, Wu HM, Cheung AY (2002) The regulation of actin organization by actin-depolymerizing factor in elongating pollen tubes. Plant Cell 14:2175–2190. DOI 10.1105/tpc.003038

Feijó JA, Sainhas J, Hackett GR, Kunkel JG, Hepler PK (1999) Growing pollen tubes possess a constitutive alkaline band in the clear zone and a growth-dependent acidic tip. J Cell Biol 144:483–496

Foissner I, Grolig F, Obermeyer G (2002) Reversible protein phosphorylation regulates the dynamic organization of the pollen tube cytoskeleton: effects of calyculin A and okadaic acid. Protoplasma 220:1–15. DOI 10.1007/s00709–002–0032–9

Fu Y, Wu G, Yang Z (2001) Rop GFPase-dependent dynamics of tip-localized F-actin controls tip growth in pollen tubes. J Cell Biol 152:1019–1032. DOI 10.1083/jcb.152.5.1019

Gibbon BC, Kovar DR, Staiger CJ (1999) Latrunculin B has different effects on pollen germination and tube growth. Plant Cell 11:2349–2363

Hamilton DA, Schwarz YH, Mascarenhas JP (1998) A monocot pollen-specific promoter contains separable pollen-specific and quantitative elements. Plant Mol Biol 38:663–669

Hanein D, Matsudaira P, DeRosier DJ (1997) Evidence for a conformational change in actin induced by fimbrin (N375) binding. J Cell Biol 139:387–396

Hepler PK, Vidali L, Cheung AY (2001) Polarized cell growth in higher plants. Annu Rev Cell Devel Biol 17:159–187. DOI 10.1146/annurev.cellbio.17.1.159

Holdaway-Clarke TL, Hepler PK (2003) Control of pollen tube growth: role of ion gradients and fluxes. New Phytol 159:539–563. DOI 10.1046/j.1469–8137.2003.00847.x

Kandasamy MK, McKinney EC, Meagher RB (1999) The late pollen-specific actins in angiosperms. Plant J 18:681–691. DOI 10.1046/j.1365-313x.1999.00487.x

Ketelaar T, Anthony RG, Hussey PJ (2004a) Green fluorescent protein-mTalin causes defects in actin organization and cell expansion in *Arabidopsis* and inhibits actin depolymerizing protein's actin depolymerizing activity in vitro. Plant Physiol 136:3990–3998. DOI 10.1104/pp.104.050799

Ketelaar T, Allwood EG, Anthony R, Voigt B, Menzel D, Hussey PJ (2004b) The actin-interacting protein AIP1 is essential for actin organization and plant development. Curr Biol 14:145–149. DOI 10.1016/j.cub.2004.01.004

Kost B, Spielhofer P, Chua NH (1998) A GFP-mouse talin fusion protein labels plant actin filaments in vivo and visualizes the actin cytoskeleton in growing pollen tubes. Plant J 16:393–401

Kovar DR, Staiger CJ, Weaver EA, McCurdy DW (2000) AtFim1 is an actin filament crosslinking protein from Arabidopsis thaliana. Plant J 24:625–636. DOI 10.1046/j.1365–313x.2000.00907.x

Kovar DR, Gibbon BC, McCurdy DW, Staiger CJ (2001) Fluorescently-labeled fimbrin decorates a dynamic actin filament network in live plant cells. Planta 213:390–395. DOI: 10.1007/s004250000494

Kuhn T, Meberg P, Brown M, Bernstein B, Minamide L, Jensen J, Okada K, Soda E, Bamburg J (2000) Regulating actin dynamics in neuronal growth cones by ADF/cofilin and Rho family GTPases. J Neurobiol 44:126–144. DOI 10.1002/1097-4695(200008)44:2 < 126::AID-NEU4 > 3.0.CO;2-Z

Laitiainen E, Nieminen KM, Vihinen H, Raudaskoski M (2002) Movement of generative cell and vegetative nucleus in tobacco pollen tubes is dependent on microtubule cytoskeleton but independent of the synthesis of callose plugs. Sex Plant Reprod 15:195–204. DOI 10.1007/s00497-002-0155-3

Lee E, Shelden EA, Knecht DA (1998) Formation of F-actin aggregates in cells treated with actin stabilizing drugs. Cell Motil Cytoskelet 39:122–133

Lovy-Wheeler A, Wilsen KL, Baskin TI, Hepler PK (2005) Enhanced fixation reveals an apical cortical fringe of actin filaments as a consistent feature of the pollen tube. Planta 221:95–104. DOI 10.1007/s00425-004-1423-2

McCann RO, Craig SW (1997) The I/LWEQ module: a conserved sequence that signifies F-actin binding in functionally diverse proteins from yeast to mammals. Proc Natl Acad Sci USA 94:5679–5684

Miller DD, Lancelle SA, Hepler PK (1996) Actin microfilaments do not form a dense meshwork in *Lilium longiflorum* pollen tube tips. Protoplasma 195:123–132

Parton R, Fischer-Parton S, Watahiki M, Trewavas A (2001) Dynamics of the apical vesicle accumulation and the rate of growth are related in individual pollen tubes. J Cell Sci 114:2685–2695

Parton R, Fischer-Parton S, Trewavas A, Watahiki MK (2003) Pollen tubes exhibit regular periodic membrane trafficking events in the absence of apical extension. J Cell Sci 116:2707–2719. DOI 10.1242/jcs.00468

Sheahan M, Rose R, McCurdy D (2004a) Organelle inheritance in plant cell division: the actin cytoskeleton is required for unbiased inheritance of chloroplasts, mitochondria and endoplasmic reticulum in dividing protoplasts. Plant J 37:379–390. DOI 10.1046/j.1365-313X.2003.01967.x

Sheahan M, Staiger CJ, Rose RJ, McCurdy DW (2004b) A green fluorescent protein fusion to actin-binding domain 2 of Arabidopsis fimbrin highlights new features of a dynamic actin cytoskeleton in live plant cells. Plant Physiol 136:3968–3978. DOI /10.1104/pp.104.049411

Taylor LP, Hepler PK (1997) Pollen germination and tube growth. Ann Rev Plant Mol Biol 48:461–491

Tsien RY (1998) The green fluorescent protein. Annu Rev Biochem 67:509–544

Twell D, Yamaguchi J, McCormick S (1990) Pollen-specific gene expression in transgenic plants: coordinate regulation of two different tomato gene promoters during microsporogenesis. Development 109:705–713

Vidali L, McKenna ST, Hepler PK (2001) Actin polymerization is necessary for pollen tube growth. Mol Biol Cell 12:2534–2545

Voigt B, Timmers ACJ, Šamaj J, Müller J, Baluška F, Menzel D (2005) GFP-FAB2 fusion construct allows in vivo visualization of the dynamic actin cytoskeleton in all cells of Arabidopsis seedlings. Eur J Cell Biol 84:595–608. DOI 10.1016/j.ejcb.2004.11.011

Wang YS, Motes CM, Mohamalawari DR, Blancaflor EB (2004) Green fluorescent protein fusions to Arabidopsis fimbrin 1 for spatio-temporal imaging of F-actin dynamics in roots. Cell Motil Cytoskelet 59:79–93. DOI 10.1002/cm.20024

Weber I, Niewöhner J, Du A, Röhrig U, Gerisch G (2002) A talin fragment as an actin trap visualizing actin flow in chemotaxis, endocytosis, and cytokinesis. Cell Motil Cytoskelet 53:136–149. DOI 10.1002/cm.10065